Tetrahedral Hohlraums at Omega

George A. Kyrala, S. R. Goldman, S. H. Batha, Jon M. Wallace,
Kenneth A. Klare, G.T. Schappert, John Oertel
Los Alamos National Laboratory

and R. E. Turner
Lawrence Livermore National Laboratory

We have initiated a study of the usefulness of tetrahedrally illuminated spherical hohlraums, using the Omega laser beams, to drive planar shocks in packages that require indirect drive. A first suite of experiments used spherical hohlraums with a 2-μm thick gold wall surrounded by a 100-μm thick epoxy layer and had an internal diameter of 2.8 mm. Four laser entrance holes each of diameter 700 μm, located on the tips of a regular tetrahedron were used. The shock velocities and the shock uniformities were measured using optical shock breakout techniques. The hohlraum x-ray radiation spectrum was also measured using a 10-channel x-ray detector. Tentatively, peak temperatures approaching 195 eV were achieved and shock speeds of 60 μm/ns were measured, when the hohlraum was driven by 22 kJ of 3ω radiation.

Introduction

Although tetrahedral hohlraums have been used on previous experiments [1] to measure implosion symmetry, little has been measured in terms of the drive strength and the usefulness of this geometry to drive packages placed on the side of the hohlraums that require uniform planar shocks. There were three goals of this initial investigation. First, measure the drive with tetrahedrally illuminated spherical hohlraums using a 10-channel x-ray detector, Dante. Second, measure the shock velocities using a streaked optical pyrometer, SOP, and test the SOP diagnostic implementation for target temperature history. Third, use the SOP, with a flat witness plate, to measure the spatial uniformity of the drive, especially looking for edge effects from the exit hole.

Target Description

The laser geometry at Omega was designed for uniform irradiation of spherical, direct drive, targets. In order to use the laser for indirect drive, either cylindrical [2] or spherical hohlraums [1] may be used. We chose the spherical hohlraums in order to maximize the amount of energy delivered to the hohlraum. The hohlraums are made of spherical shells of plastic epoxy, 100 μm thick, with a 2 μm layer of gold plated on the inside. The spheres have an internal diameter of 2.8 mm. Laser entrance holes were placed at the apex of a regular tetrahedron to maximize the number of beams inside the hohlraums. The laser entrance holes had a diameter of 700 μm. The laser beam pointing and focusing were adjusted to minimize the non-uniformity in illumination of the package, to avoid being close to the planar package, and to maximize the uniformity of illumination on the wall of the hohlraum. Conical shields were placed around the packages on the outside of the hohlraum to shield the packages and the diagnostics from the hohlraum radiation, and from the light emission from the laser entrance holes, *figure 1*.

Up to fifteen laser beams may be incident on each hole, however only twelve were used in this study. The other laser beams were dedicated to x-ray backlighting. Two different laser beam pulse shapes were used: a 1- ns square laser pulse to drive shocks, and a shaped (PS-26) laser pulse useful for Raleigh-Taylor growth experiments.

The expected temperature in a gold hohlraum is given by $T_R(eV)=75.3\ E_L(kJ)^{1/3}$ [3] with a 65% x-ray conversion efficiency. It was expected that shocks could be driven in an aluminum witness to a speed of 55 μm/ns, with a peak pressure of 45 Mbar using a 2-ns long square laser pulse.

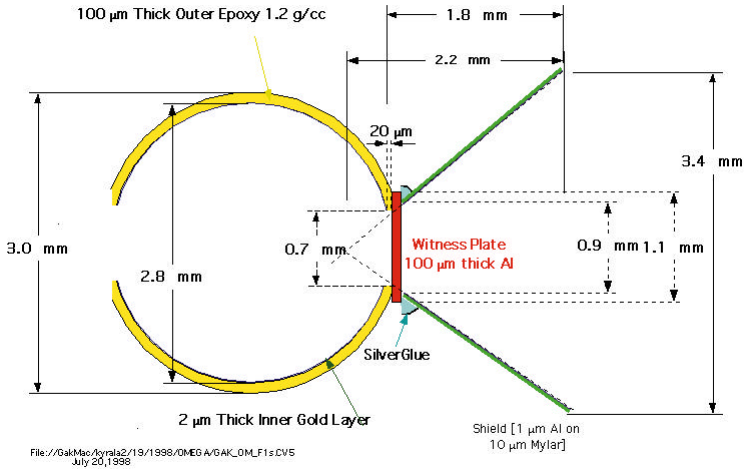

Figure 1. Schematic diagram of the target with a witness plate and a conical shield for the SOP diagnostic

In designing these planar experiments, we faced two conflicting requirements; we needed as much of the laser energy as possible to drive the shocks, but we also needed sufficient laser energy to produce x-ray backlighting images. We estimated that at least 10 beams [4.5 kJ of 3ω light] would be needed to register an image of a 500-μm-thick C_8H_7Cl target on an x-ray framing camera set at medium gain and with a magnification of 10 using an Iron He-α like backlighter. The second conflict is that of creating a sufficiently large area shock front, to drive as uniform a shock as possible. X-ray backlighting will not be needed if the SOP can measure the spatial variation in the shock front with sufficient resolution for future experiments. If x-ray backlighting is not needed, then these ten beams may be used to heat the hohlraum hotter and drive stronger shocks.

SOP Description

A streaked optical spectrometer, SOP, was used and has been described earlier [4]. Briefly, it consists of an f/7 telescope with a 6-mm field of view that collects the light from the back of a foil and images it at the entrance of a streak camera. The SOP light is filtered by a narrow band filter to select in the UV that excludes the scattered light from the laser. The SOP telescope has a magnification of 11.7x, and has a measured static optical resolution of 7-μm per line pair, and a temporal resolution of 10 ps limited by the CCD recording medium.

Shock Speed Simulations

The shock speed in the aluminum witness plate was calculated using the radiation hydro-code Lasnex, The radiation drive was determined using a one-dimensional spherical hohlraum calculation with Pn radiation transport, the appropriate laser deposition source, a term for laser entry hole radiation losses, and an aluminum sphere at the hohlraum center with surface area equal to the surface area of the aluminum drive plate subtended by the defining hole in the hohlraum wall, *figure 2*

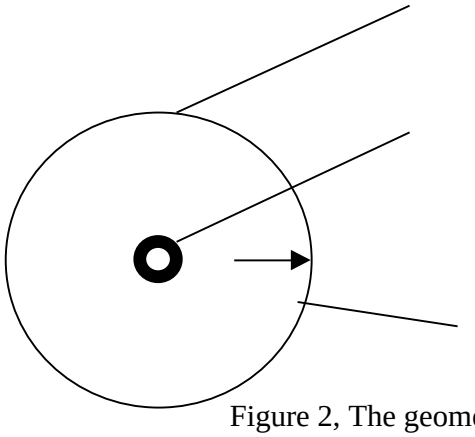

Figure 2, The geometry used for the calculations

The radii of the hohlraum and the aluminum shells were scaled up in linear dimension by a factor of 10 so that convergence effects would be minimized for the shock in aluminum, and the density of material in the hohlraum between the aluminum sphere and the hohlraum shell was made extremely low to avoid making the hohlraum volume an erroneously large energy sink; correspondingly the incident laser energy and the energy loss due to the laser entry holes were increased by a factor of 100. Hence the shock motion in the aluminum shell was determined as part of a single lasnex calculation.

The hohlraum radiation temperature obtained from the above lasnex calculations were used as the source in a two-dimensional Rage calculation that modeled both a section of the hohlraum wall and the aluminum witness plate mounted on it. There were no geometric convergence effects in the direction of shock propagation, although the two-dimensional modeling of the hohlraum wall section and the planar target allowed for the calculation of rarefaction effects due to the finite size of the aluminum witness plate surface transverse to the direction of shock motion. The lasnex and the Rage results agree, indicating that geometric convergence effects in the lasnex calculation were not significant. An example of the pressure variation in the aluminum as a function of time is shown in *figure 3*, which presents results for shock propagation though a planar target using the radiation drive calculated from the spherical one-dimensional lasnex simulations.

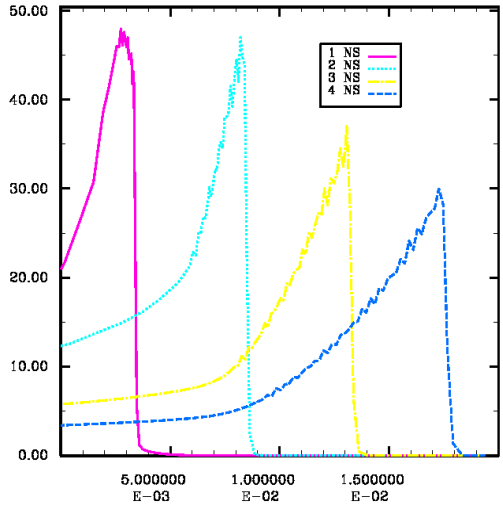

Figure 3. The pressure as a function of position at times from 1 to 4 ns from a planar Lasnex calculation of the shock propagation in aluminum, with a peak temperature of 200 eV.

Shock Speed Results

The data from the SOP consist of three types: uniformity of the drive, shock arrival times from a stepped target, and time history from a wedge that varies in thickness. We used flat 100-μm thick aluminum witness plates to test the uniformity of the drive. The witness plate covered the hole facing the SOP diagnostics. The plates were shielded by plastic-covered aluminum cones. This reduced the scattered light and shielded the SOP from the light emission form the laser entrance holes. The cone extended 100 μm beyond the projected circumference of the hohlraum. With 60 heating beams, shots 13662 and 13663, [30 and 23.85 kJ respectively] gave a 600-μm diameter region with an arrival time of the shock varying less than 20 ps for transit times of about 800-ps and 1536-ps respectively. This corresponds to a uniformity of pressure of 2.5 and 1.25 % respectively. When the drive energy was lowered to 21.4 kJ by using only 45, the region was observed to have similar uniformity in drive pressure. An example of the emission uniformity is shown in *figure 4*.

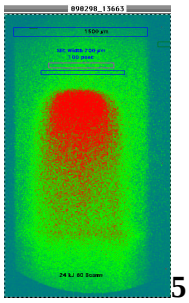

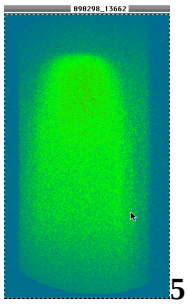

24 kJ **30 kJ**

Figure 4. Uniformity of the drive at incident laser energies of 24 kJ, left figure, and 30 kJ, right figure, for an aluminum witness plate**.**

The shock transit time was also measured with aluminum and Be-doped Cu step wedges. The measured average speed across the first step, was 55 μm/ns, measured at 21 kJ incident laser energy. The measured average speed across the second step was less, indicating a slowing down of the shock as it propagates. The hohlraum temperature derived from the shock speed is 222 eV assuming the Sesame EOS for aluminum and using the scaling of the shock speed with pressure and hence temperature, $T_R(eV) \sim 16.8\ U_s(\mu m/ns)^{0.62}$ [3].

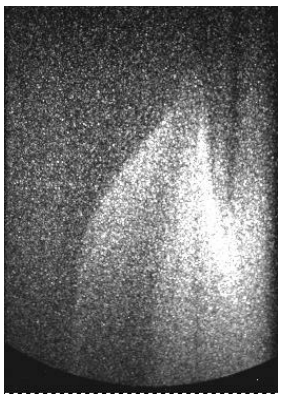

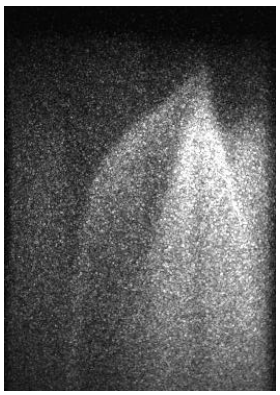

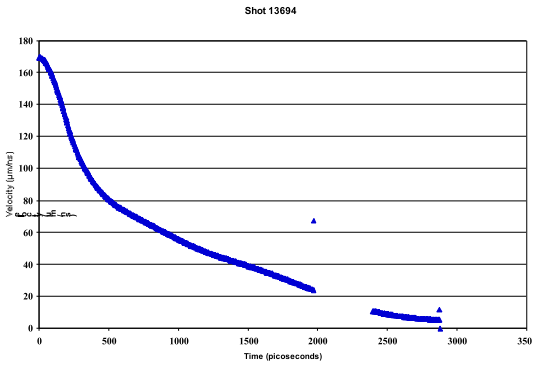

Pulse shape 26 Square wave drive Square pulse History

Figure 5. Example of the emission recorded by the SOP for aluminum witness pates driven by pulse shape 26 and a square laser pulse. Time increases from top to bottom and the horizontal axis is the spatial direction. A record of the emission speed for the square pulse is also shown.

Another measure of the drive history can be deduced from the wedge data. A typical example of the SOP data recorded for the square pulse and for a pulse shape26 is shown in *figure 5*. The figures show the change in the instantaneous velocity with time. This velocity, however, is that of the emission at a given brightness temperature, and is less accurate than a step wedge measurement. The large velocities at short times are an artifact of the inaccuracy in the position of zero time and should not be trusted. Note that the differences in breakout for different kinds of drive show clearly in the streak records.

X-Ray Measurements

The thermal radiation temperature, T_R , was measured using the Dante diagnostic [5,6] a 10-channel array of absolutely calibrated x-ray detectors, viewing the hohlraum through two of the LEHs. In principle, Dante samples the same radiation field that the planar package

samples. The Dante field of view includes a mix of irradiated and non-irradiated wall areas and LEH areas similar to what the capsule would see. Consequently, no "albedo corrections" [2] to the data were made. The only corrections were for the effective LEH emission area due to the non-normal viewing. T_R is then based on a source size of 700-um diameter @ 21.8 degrees, plus a second source of 700-um diameter at 70.5 degrees. No corrections for laser hot spots, LEH loss, or finite wall thickness at the LEH (this latter one may be important for the small contribution at 70.5 degree) have been made yet.

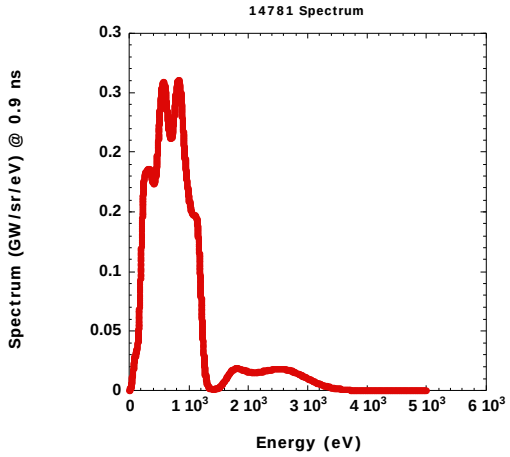

Figure 6
De-convolved spectrum from for shot 14781 with a square pulse shape and 22.5 kJ incident laser energy.

The radiation spectrum emitted by the hohlraum is naturally separated into two parts, *figure 6*; the thermal part below 1.5-keV, and the above 1.5 keV that arises from the M-band emission of the gold wall. We use the part of the spectrum below 2-keV and we account for the effective source size that Dante observes to define a hohlraum temperature. The de-convolved temperature measurements are shown in *figure 7* for the two different pulse shapes.

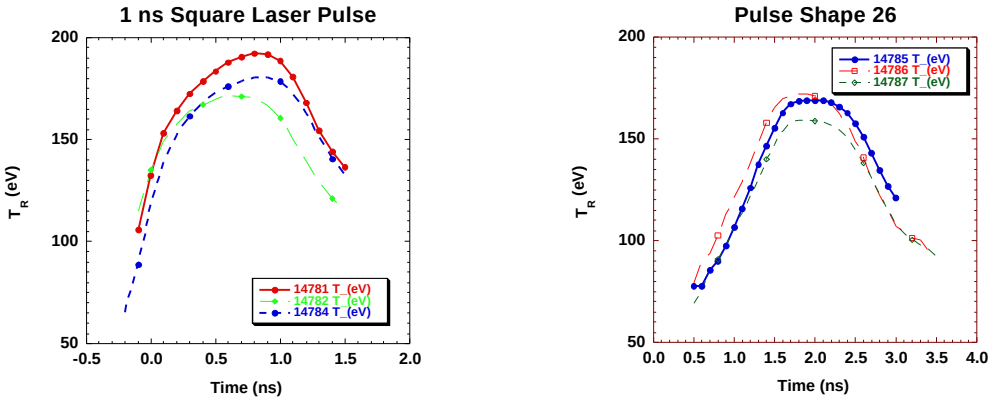

Figure 7. The hohlraum radiation temperature of two different laser pulse shapes and various laser energies. The time axis is referenced arbitrarily.

Scaling

The scaling of the measured temperature with laser energy is depicted in *figure 8*. The hohlraum radiation temperature behaves like the square root laser energy, in contrast to the one-third power that is typically predicted [3] inside a cylindrical hohlraum. We find, in agreement with Lindl [7], that an efficiency of 65 % is needed to make the data fit the prediction from the simple energy scaling formulas. If we include the data taken previously [1] with a different set of hohlraums and orientations at higher laser energies [using 60 beams] the scaling continues to behave as $E^{1/2}$ as well.

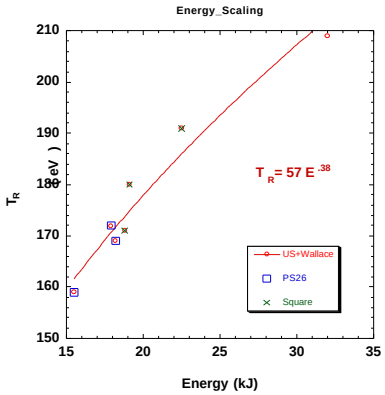

Figure 8
Energy scaling of a tetrahedral hohlraum with incident laser energy for two different pulse shapes. The point at 32 kJ from reference 1.

Summary

Previous measurements [1] used a tetrahedral hohlraum of diameter 2.8-mm with 700-μm diameter LEHs driven by a square laser pulse. When driven by 32 kJ in 60 beams, a hohlraum temperature of 209 eV was measured, with an SBS backscatter fraction of 3.4. This paper reports the use of similarly sized hohlraums to drive planar packages. Hohlraum temperatures of up to 195 eV were measured using a multi-channel x-ray diagnostic while temperatures up to 222 eV were measured using a shock breakout technique on different shots. For the experiments reported here, the SBS backscatter fraction was measured to be in the 3 to 8 % range for the 1-ns square pulses and 2 to 11 % for the PS-26 pulses. No measurements were made of the amount of energy backscattered due to SRS. We have used tetrahedrally illuminated spherical hohlraums to drive planar packages. We demonstrated that up to 195 eV drive could be used to generate up to 50 Mbar shocks and to drive planar shocks uniformly over a 600-μm diameter spot in aluminum.

Acknowledgements

This work was supported by the U.S. DOE under contract no. W7405-ENG-36. We would like to thank the Omega crew, the Los Alamos Operations Team, and the Los Alamos Target Fabrication Team for excellent support.

References

[1] J. M. Wallace, T. J. Murphy, N. D. Delamater, K. A. Klare, J. A. Oertel, G. R. Magelssen, E. L. Lindman, A. A. Hauer, and P. Gobbby, J. D. Schnittman, R. S. Craxton, W. Seka, R. Kremens, and D. Bradley, S. M. Pollaine, R. E. Turner, and O. L. Landen, D. Drake, J. J. MacFarlane, Inertial Confinement Fusion with Tetrahedral Hohlraums at OMEGA, Phys. Rev. Lett. 82, 3807-3811 (1999).

[2] C. Decker, R. E. Turner, O. L. Landen, L. J. Suter, P. Amendt, H. N. Kornblum, and B. A. Hammel, T. J. Murphy, J. Wallace, N. D. Delamater, P. Gobby, A. A. Hauer, G. R. Magelssen, and J. A. Oertel, J. Knauer, F. J. Marshall, D. Bradley, W. Seka, and J. M. Soures, Hohlraum Radiation Drive Measurements on the Omega LaserPhys Rev. Lett. 79, 1491-1495 (1997).

[3] R. L. Kauffman, H. N. Kornblum, D. W. Phillion, C. B. Darrow,, B. F. Lasinski, L. J. Suter, A. R. Thiessen, R. J. Wallace, and F. Ze Drive characterization of indirect drive targets on the Nova laser, Rev. Sci. Instr. 66, 678-681 (1995).

[4] J. A. Oertel, T. J. Murphy, R. R. Berggen, J. Faulkner, R. Schnell, D. Little, T. A. Archuleta, J. Lopez, and J. Velarde, A Multipurpose TIM-Based Optical Telescope for Omega and the Trident Laser Facilities, Rev. Sci. Instr. 70,803-805,(1999).

[5] H. N. Kornblum, R. L. Kauffman, and J. A. Smith, Rev. Sci. Instrum. 57, 2101 (1986).

[6] R. L. Kauffman, L. J. Suter, C. B. Darrow, J. D. Kilkenny, H. N. Kornblum, D. S. Montgomery, D. W. Phillion, M. D. Rosen, A. R. Thiessen, R. J. Wallace, and F. Ze, High Temperatures in Inertial Confinement Fusion Radiation Cavities Heated with 0.35 μm Light Phys. Rev. Lett. 73, 2320 (1994).

[7] J. Lindl, Inertial Confinement Fusion, AIP press, New York, 1998.